Transaction B: Mechanical Engineering
Vol. 16, No. 1, pp. 1–14

SCIENTIA IRANICA

On the Kinematic Analysis of a Spatial Six-Degree-of-Freedom Parallel Manipulator

M. Vakil[1], H. Pendar[1] and H. Zohoor[1,*]

Abstract. *In this paper, a novel spatial six-degree-of freedom parallel manipulator actuated by three base-mounted partial spherical actuators is studied. This new parallel manipulator consists of a base platform and a moving platform, which are connected by three legs. Each leg of the manipulator is composed of a spherical joint, prismatic joint and universal joint. The base-mounted partial spherical actuators can only specify the direction of their corresponding legs. In other words, the spin of each leg is a passive degree-of-freedom. The inverse pose and forward pose of the new mechanism are described. In the inverse pose kinematics, active joint variables are calculated with no need for evaluation of the passive joint variables. To solve the forward pose problem, a much simpler method compared to the traditional method is introduced. Closed form relations for the inverse and forward rate kinematics are proposed. Finally, two sets of singular configuration of the newly introduced manipulator with different natures are obtained.*

Keywords: *Inverse kinematics; Forward kinematics; Rate kinematics; Parallel mechanism; Singular configuration.*

INTRODUCTION

There have been great developments in the field of parallel manipulators over the past decade. The parallel manipulators have several advantages compared to serial robots, such as: high stiffness, high speed, large load carrying capacity and precision positioning. However, compared to serial manipulators, parallel manipulators suffer from reduced workspace and a complicated forward kinematics analysis.

Many designs of parallel manipulators with specific actuation ways and Degrees-Of-Freedom (DOF) have been introduced by researchers over the past two decades. Stewart [1] designed a general six legs platform-manipulator as an airplane simulator. Hunt [2] used the Stewart platform as a robotic manipulator. Romiti and Sorli [3] proposed a 6-DOF parallel robot named TuPaMan. Beli [4] investigated a 6-DOF manipulator, which consisted of three PRPS legs. Hudegns and Tear [5] introduced a 6-DOF parallel manipulator, in which the six inextensible legs were driven by a four-bar mechanism located on the ground. Jongwon et al. [6] presented a 6-DOF manipulator named Eclipse-II, which allowed a 360 degree spinning of the platform. Williams and Polling [7] proposed a novel 6-DOF spherically actuated platform manipulator with only two legs. There is much more research in the area of parallel manipulators [8-11]. Also, an atlas of parallel robots, created by Merlet, can be found at http://www.inria.fr/personnel/merlet/merlet_eng.html.

The novel 6-DOF manipulator studied in the present article has three legs [12]. Each leg consists of a spherical joint, a prismatic joint and universal joints (SPU). These three legs connect the equilateral moving triangle (moving platform) to the equilateral fixed triangle (base platform). Each leg has a partially actuated spherical actuator. The spherical actuator of each leg can only specify the direction of the leg. Thus, the spin of the leg is a passive variable. (It is worth mentioning that each spherical actuator, if fully actuated, can specify the direction, as well as the spin, of the leg [13].) A spherical motor has been built by Lee et al. [14]. Also, there is another type of spherical motor introduced by Wang et al. [15].

The introduced manipulator here is based on the two-leg spherically actuated manipulator designed in [7], which is completely analyzed in [16]. The specific feature of the two-leg spherically actuated manipulator [7,16] is that, with only two legs, it has

1. *Department of Mechanical Engineering, Sharif University of Technology, P.O. Box 11155-9567, Tehran, Iran.*
*. *Corresponding author. E-mail: zohoor@sharif.edu*

Received 12 February 2006; received in revised form 30 September 2007; accepted 10 March 2008

6 DOF. Fewer legs lead to a smaller required space for the manipulator's installation, decrease the chance of leg collisions during maneuver and, also, mean fewer moving parts. However, the rigidity of the manipulator in [7] is not high. To increase the rigidity of the two-leg spherically actuated platform manipulator, the three-leg partially actuated spherical manipulator, as suggested in [7, p. 156], which is the subject of this research paper, is proposed [17]. Although the three-leg partially actuated spherical manipulator has an extra leg compared to the two-leg manipulator, in comparison to the other well-known 6-DOF manipulators, like the Stewart manipulator, it has fewer legs. Moreover, due to the existence of three spherical actuators, there are several different actuation ways for the manipulator, as discussed in [13]. Therefore, by combining these different actuation ways, it might be possible to design a singularity free parallel manipulator. Although, in this article, just one actuation way in which the spherical actuator specifies the direction of the corresponding leg is analyzed, the existence of several different actuation ways is another benefit of the newly introduced manipulator. It is to be noted that, as discussed in [7], the SPU leg manipulator suffers from a low load-carrying capacity, which is a direct consequence of its actuation. Moreover, in the presence of an external load on the moving manipulator (or even because of the weight of the platform and legs), there will be unavoidable moments on the legs. These moments should be compensated by the actuator inputs. Nonetheless, other mechanisms actuated by R-joints suffer from such a deficiency as well.

In this paper, the inverse and forward poses and rate kinematics of the novel mechanism are studied. In the inverse pose problem, active joint variables are calculated, with no need for evaluation of the passive joint variables. In the forward pose problem, a much simpler method compared to the traditional approach is introduced. To tackle the forward problem through the traditional approach, one has to solve twelve nonlinear equations, which are obtained by equating the transformation matrices between the moving platform and the base platform through each leg. However, the new method for the forward pose problem introduced here requires the solution of only three nonlinear equations with less nonlinearity. Moreover, closed form relations for the inverse and forward rate kinematics are obtained. Finally, the singular configurations of the introduced mechanism, with their physical interpretations, are analyzed.

First, in the following section, the novel manipulator is described. Then, the inverse and forward poses, as well as the inverse and forward rate kinematics, are demonstrated. After that, the singular configurations of the mechanism are discussed. Finally, the conclusion of the research is presented.

MECHANISM AND COORDINATE DESCRIPTION

Mechanism Description

The parallel manipulator studied in the present article consists of a moving platform connected to the base platform by three legs. The moving platform and base platform are both equilateral triangles (Figure 1). Each leg is composed of a spherical joint, a prismatic joint and a universal joint, which is called a SPU leg. These joints construct each leg in a serial manner (Figure 2).

Although the manipulator consists of three legs, it has 6-DOF. This is proven through the Grubler formula, as stated below:

$$F = 6(l - n - 1) + \sum_{i=1}^{n} f_i,$$

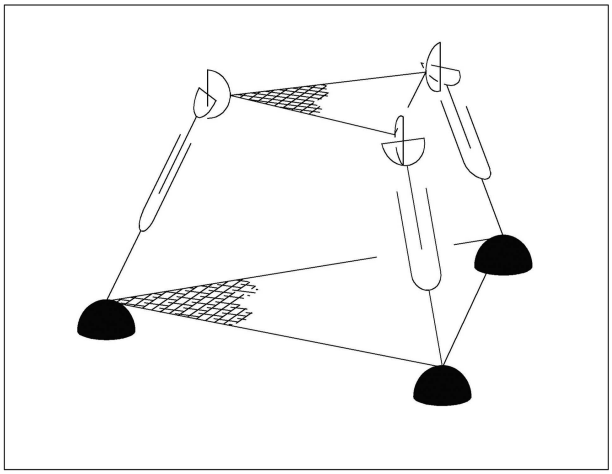

Figure 1. Schematic of the introduced 6 DOF manipulator with three SPU legs.

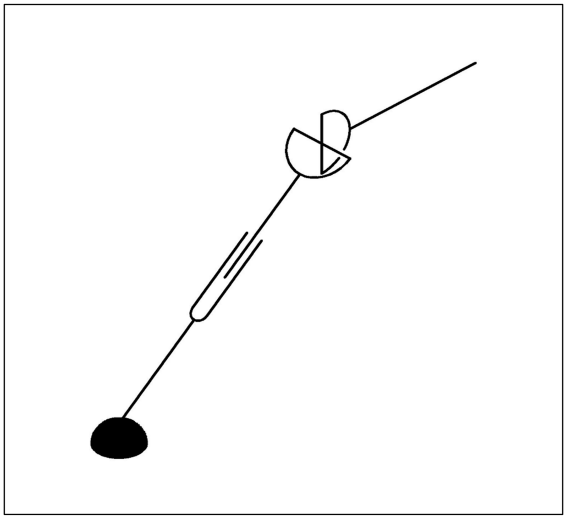

Figure 2. Schematic of each SPU leg of the introduced 6 DOF manipulator.

where l is the number of links (including base), n is the number of joints, and f_i is the DOF of the ith joint. Therefore, using the Grubler formula, we have:

$$F = 6(8 - 9 - 1) + 3(3) + 3(1) + 3(2) = 6.$$

The actuation of the mechanism is through the spherical joints and spherical actuators. The spherical actuators are partially active, since they can only specify the directions of their leg. In other words, the spin of the leg is a passive variable.

Parameters and Coordinate Description

For the base platform, as well as the moving platform, a coordinate frame is assigned. The origins of the moving platform coordinate frame and base platform coordinate frame are at the geometrical centers of the equilateral triangles, which construct the moving platform and base platform, respectively. The moving platform coordinate frame, P, base platform coordinate frame, B, as well as the legs' numbering, are schematically shown in Figure 3.

To specify the location and orientation of the moving platform coordinate frame, with respect to the base platform coordinate frame, the following transformation matrix is considered.

$$
{}^{B}_{P}T = \begin{bmatrix}
\cos(\alpha)\cos(\beta) & \cos(\alpha)\sin(\beta)\sin(\gamma) - \sin(\alpha)\cos(\gamma) & \cos(\alpha)\sin(\beta)\cos(\gamma) + \sin(\alpha)\sin(\gamma) & x \\
\sin(\alpha)\cos(\beta) & \sin(\alpha)\sin(\beta)\sin(\gamma) + \cos(\alpha)\cos(\gamma) & \sin(\alpha)\sin(\beta)\cos(\gamma) - \cos(\alpha)\sin(\gamma) & y \\
-\sin(\beta) & \cos(\beta)\sin(\gamma) & \cos(\beta)\cos(\gamma) & z \\
0 & 0 & 0 & 1
\end{bmatrix}. \quad (1)
$$

It is to be noted that the rotation part of the above transformation matrix is based on the $Z - Y - X$ Euler angles. Moreover, for each leg, the standard Denavit-Hartenberg coordinate frames are assigned and the corresponding Denavit-Hartenberg parameters are obtained. In assigning the Denavit-Hartenberg coordinate frame, for each revolute and prismatic joint, a coordinate frame should be defined. If the joint is neither prismatic nor revolute, it has to be decomposed into these two base joints. For instance, the spherical joint should be decomposed into three revolute joints, in which the rotating axes of the revolute joints are mutually orthogonal to each other. A schematic of the Denavit-Hartenberg coordinate frames for a spherical joint is shown in Figure 4. In this figure, θ_1, θ_2 and θ_3 represent the roll, yaw and pitch angles of the spherical joint.

Also, the universal joint will be decomposed into two revolute joints, in such a way that the axes of the rotations of the revolute joints are orthogonal to each other. A schematic of the Denavit-Hartenberg coordinate frames for the universal joint is shown in Figure 5.

The assigned Denavit-Hartenberg coordinate frames for each leg are shown in Figure 6.

The constant platform parameters, as well as the Denavit-Hartenberg parameters for each leg of the manipulator, are as follows:

L_B:	Distance between two spherical joints (or side length of the base platform),
L_P:	Distance between two universal joints (or side length of the moving platform),
l_i:	Length of the ith leg,
$(\theta_{1i}, \theta_{2i}, \theta_{3i})$:	Spherical joint variables for the ith leg,

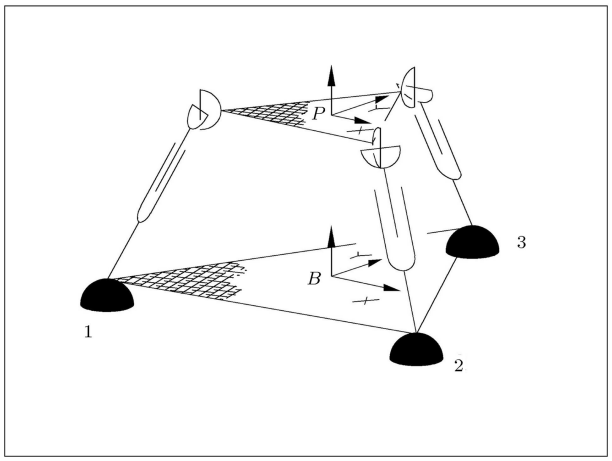

Figure 3. Schematic of the base and platform coordinate frames and legs' numbering.

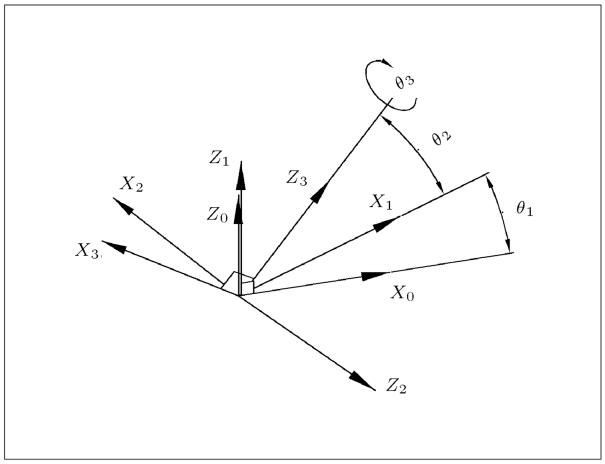

Figure 4. Denavit-Hartenberg coordinate frames of the spherical joint of the SPU leg.

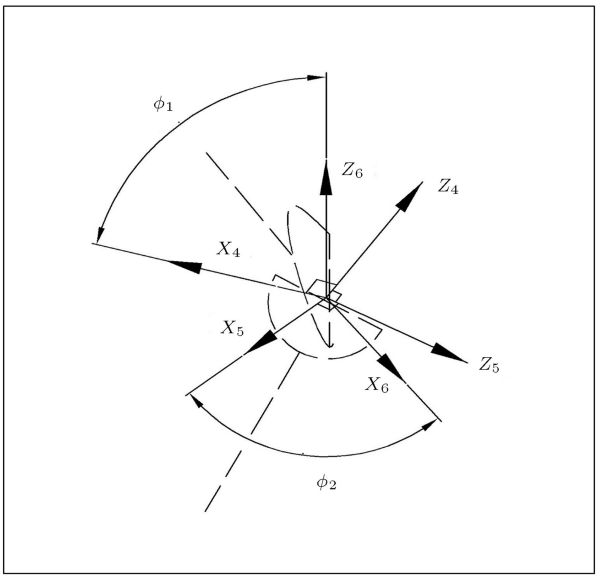

Figure 5. Denavit-Hartenberg coordinate frames of the universal joint of the SPU leg.

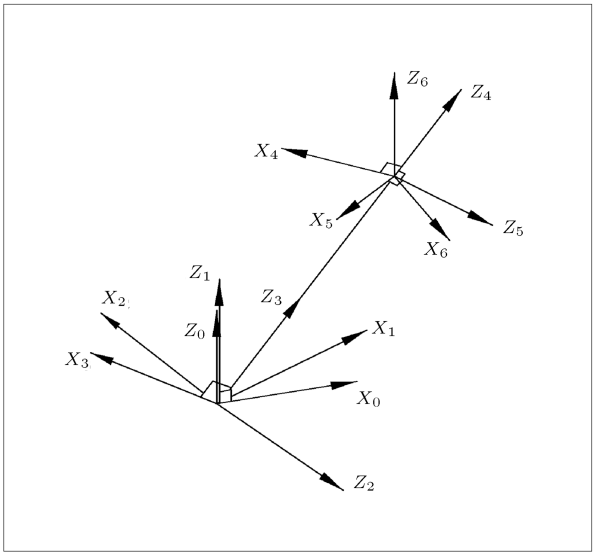

Figure 6. Denavit-Hartenberg coordinate frames of each SPU leg.

(ϕ_1, ϕ_{2i}): Universal joint variables for the ith leg,

In Figures 4, 5 and 6, the X and Z axes for the Denavit-Hartenberg coordinate frames are shown and the Y-axis can be easily obtained via the right-hand rule.

KINEMATICS

Inverse Pose Solution

In the inverse pose procedure, the active joint variables should be calculated, having ${}^{P}_{B}T$. The active variables for each leg are $(\theta_{1i}, \theta_{2i})i = 1 \cdots 3$ and the third spherical joint variable of each leg, $(\theta)_{3i}i = 1 \cdots 3$, is passive. The numbering of the legs is shown in Figure 3.

The transformation matrix between coordinate frame "0" and coordinate frame "6" of each leg, shown in Figure 6, can be calculated using the Denavit-Hartenberg parameters presented in Table 1. This transformation matrix is:

$$({}^{0}_{6}T)_i = ({}^{0}_{1}T)_i({}^{1}_{2}T)_i({}^{2}_{3}T)_i({}^{3}_{4}T)_i({}^{4}_{5}T)_i({}^{5}_{6}T)_i, \tag{2}$$

where $({}^{k-1}_{k}T)_i$ is the transformation matrix between coordinates k and $k-1$ of the ith leg. $({}^{0}_{6}T)_i$ can also be obtained as:

$$({}^{0}_{6}T)_i = ({}^{B}_{0}T)^{-1}_i \, {}^{B}_{P}T ({}^{6}_{P}T)^{-1}_i, \tag{3}$$

where $({}^{B}_{0}T)_i$ and $({}^{6}_{P}T)_i$ for each leg were given in the Appendix. In the inverse kinematics, ${}^{B}_{P}T$ is given. Also, $({}^{0}_{B}T)_i$ and $({}^{6}_{P}T)_i$ are known, since the platform Therefore, from Equation 3, $({}^{0}_{6}T)_i$ is known. Equating the fourth column of Equations 2 and 3 leads to:

$$\overbrace{\begin{bmatrix} k_{1i} \\ k_{2i} \\ k_{3i} \\ 1 \end{bmatrix}}^{\text{fourth column of Equation 3}} = ({}^{B}_{0}T)^{-1}_i \, {}^{B}_{P}T ({}^{6}_{P}T)^{-1}_i \begin{bmatrix} 0 \\ 0 \\ 0 \\ 1 \end{bmatrix} = \overbrace{\begin{bmatrix} l_i \cos(\theta_{1i}) \cos(\theta_{2i}) \\ l_i \sin(\theta_{1i}) \cos(\theta_{2i}) \\ l_i \sin(\theta_{2i}) \\ 1 \end{bmatrix}}^{\text{fourth column of Equation 2}}. \tag{4}$$

Thus, from Equation 4, the active spherical joint variables for each leg are as follows:

θ_{2i} is:

$$\theta_{2i} = \text{asin}\ (k_{3i}/l_i), \tag{5}$$

and θ_{1i} is:

$$\theta_{1i} = \text{atan}\ 2(k_2, k_1) \qquad \text{if } \cos(\theta_2) > 0, \tag{6a}$$

$$\theta_{1i} = \text{atan}\ 2(-k_2, -k_1) \qquad \text{if } \cos(\theta_2) < 0, \tag{6b}$$

where atan 2 is the inverse tangent function considering the sign of its components and asin is the arcsin. It is worth mentioning that, for $\cos(\theta_2) = 0$, Equations 6a

Table 1. Denavit-Hartenberg parameters for the each leg.

i	α_{i-1}	a_{i-1}	d_i	θ_i
1	0	0	0	θ_1
2	90	0	0	$\theta_2 + 90$
3	90	0	0	θ_3
4	0	0	ℓ_f	0
5	-90	0	0	$90 - \phi_1$
6	90	0	0	ϕ_2

and 6b are not valid, since $\cos(\theta_2) = 0$ leads to a singular configuration of the mechanism, as discussed in the following sections. The active joint variables for each leg are θ_{2i} and θ_{1i}. In the following, θ_{3i}, which is a passive variable, will be evaluated. (A reason for introducing the procedure of calculating θ_3 here is that this procedure will be used in the section of "Forward Pose Solution".) To calculate other passive variables, l_i and ϕ_{1i}, ϕ_{2i}, an approach similar to [7] can be adopted (See Equations 4 and 5 in [7]). Having θ_{1i} and θ_{2i}, then, Z_{3i} is:

$$^{B}(Z_{3i}) = \begin{bmatrix} \cos(\theta_{1i})\cos(\theta_{2i}) \\ \sin(\theta_{1i})\cos(2i) \\ \sin(\theta_{2i}) \end{bmatrix}. \quad (7)$$

Also, Z_{6i} can be derived from the third column of $(^{0}_{6}T)_i$, which is:

$$^{B}(Z_{6i}) =$$

$$\begin{bmatrix} (-\cos(\theta_{1i})\sin(\theta_{2i})\cos(\theta_{3i}) \\ \quad + \sin(\theta_{1i})\sin(\theta_{3i}))\cos(\phi_{1i}) \\ \quad + \cos(\theta_{1i})\cos(\theta_{2i})\sin(\varphi_{1i}) \\ (-\sin(\theta_{1i})\sin(\theta_{2i})\cos(\theta_{3i}) \\ \quad - \cos(\theta_{1i})\sin(\theta_{3i}))\cos(\phi_{1i}) \\ \quad + \sin(\theta_{1i})\cos(\theta_{2i})\sin(\phi_{1i}) \\ \cos(\theta_{2i})\cos(\theta_{3i})\cos(\phi_{1i}) + \sin(\theta_{2i})\sin(\phi_{1i}) \end{bmatrix}. \quad (8)$$

Cross producing $^{B}(Z_{3i})$ and $^{B}(Z_{6i})$, which are given in Equations 7 and 8, respectively, results in:

$$^{B}(Z_{3i}) \times {}^{B}(Z_{6i}) =$$

$$\begin{bmatrix} \cos(\phi_{1i})\sin(\theta_{1i})\cos(\theta_{3i}) \\ \quad + \sin(\theta_{2i})\cos(\phi_{1i})\cos(\theta_{1i})\sin(\theta_{3i}) \\ -\cos(\phi_{1i})\cos(\theta_{1i})\cos(\theta_{3i}) \\ \quad + \sin(\theta_{2i})\cos(\phi_{1i})\sin(\theta_{1i})\sin(\theta_{3i}) \\ -\cos(\theta_{2i})\cos(\phi_{1i})\sin(\theta_{3i}) \end{bmatrix}. \quad (9)$$

Multiplying both sides of Equation 9 by:

$$(^{2}_{0}R)_i = (^{0}_{1}R^{1}_{2}R)^{-1}_{i} =$$

$$\begin{bmatrix} -\cos(\theta_{1i})\sin(\theta_{2i}) & -\sin(\theta_{1i})\sin(\theta_{2i}) & \cos(\theta_{2i}) \\ -\cos(\theta_{1i})\cos(\theta_{2i}) & -\sin(\theta_{1i})\cos(\theta_{2i}) & -\sin(\theta_{2i}) \\ \sin(\theta_{1i}) & -\cos(\theta_{1i}) & 0 \end{bmatrix}, \quad (10)$$

leads to:

$$(^{2}_{0}R)_i(^{B}(Z_{3i}) \times {}^{B}(Z_{6i})) = \begin{bmatrix} -\sin(\theta_{3i})\cos(\phi_{1i}) \\ 0 \\ \cos(\theta_{3i})\cos(\phi_{1i}) \end{bmatrix}. \quad (11)$$

Or, equally:

$$(^{2}_{0}R)_i(^{B}(Z_{3i}) \times {}^{B}(Z_{6i})) = \begin{bmatrix} d_{1i} \\ d_{2i} \\ d_{3i} \end{bmatrix}. \quad (12)$$

Since θ_{1i} and θ_{2i} are already calculated, $^{B}(Z_{3i})$ and $(^{2}_{0}R)_i$ are known. Also, $^{B}(Z_{6i})$, which relates to the third column of $(^{0}_{6}T)_i$, can be obtained. Thus, the left hand side of Equation 12 is completely known. Equating Equations 11 and 12, θ_{3i} is:

$$\theta_{3i} = \text{atan2}(-d_{1i}, d_{3i}). \quad (13)$$

It is worth noting that, if $\phi_{1i} = \pm 90$, then, $\cos(\phi_{1i}) = 0$ and Equation 13 are not applicable. This is due to the fact that $\phi_{1i} = \pm 90$ leads to a singular configuration for the introduced mechanism, as discussed in the following section. Since Equations 5 and 13 for θ_{2i}, θ_{3i} are in the asin and atan 2 formats, it can be concluded that there are four possible sets for θ_{1i}, θ_{2i}, θ_{3i}, ϕ_{1i} and ϕ_{2i}. That is, there are four different sets of θ_{1i}, θ_{2i}, θ_{3i}, ϕ_{1i} and ϕ_{2i}, which lead to the same location and orientation of the ith leg. For example, in Figure 7, the pair (θ_1, θ_2) and the pair $(\theta_1 + \pi, \pi - \theta_2)$ result in the same direction for line η.

Different sets of θ_{1i}, θ_{2i}, θ_{3i}, ϕ_{1i} and ϕ_{2i} for the ith leg are given in Table 2. Since there are four sets for θ_1, θ_2, θ_3, ϕ_1 and ϕ_2 of each, there are 64 possible sets of θ_{1i}, θ_{2i}, θ_{3i}, ϕ_{1i} and $\phi_{2i} (i = 1 \cdots 3)$ for the inverse problem, which all correspond to one configuration of the mechanism.

The inverse pose problem of the introduced mechanism is solved for the following two cases and only the first set in Table 2 is provided. In calculating the

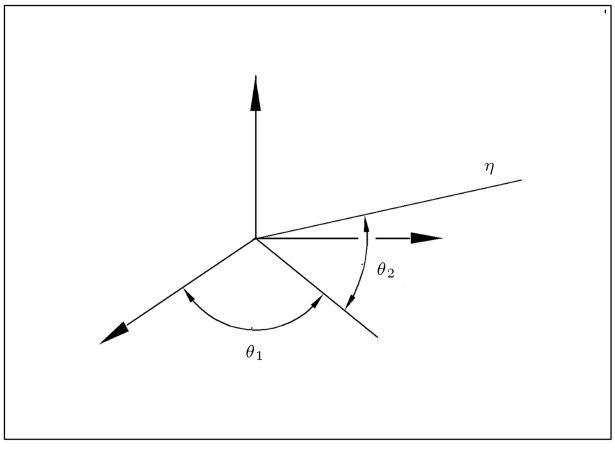

Figure 7. Schematic of θ_1, θ_2 of each SPU leg of the introduced 6 DOF manipulator.

Table 2. Multiple sets for inverse solution of the each leg.

First set	θ_{1i}	θ_{2i}	θ_{3i}	ϕ_{1i}	ϕ_{2i}
Second set	θ_{1i}	θ_{2i}	$\theta_{3i}+\pi$	$\phi_{1i}+\pi$	$\phi_{2i}+\pi$
Third set	$\theta_{1i}+\pi$	$\pi-\theta_{2i}$	θ_{3i}	ϕ_{1i}	$\phi_{2i}+\pi$
Froth set	$\theta_{1i}+\pi$	$\pi-\theta_{2i}$	$\theta_{3i}+\pi$	$\phi_{1i}+\pi$	ϕ_{2i}

following variables, $L_P = 20$ cm and $L_B = 30$ cm were assumed.

$$\begin{cases} x = 0 \\ y = 5 \text{ cm} \\ z = 5 \text{ cm} \\ \alpha = 10^\circ \\ \beta = 10^\circ \\ \gamma = 10^\circ \end{cases} \Rightarrow \begin{cases} \theta_{11} = 15.93^\circ \\ \theta_{12} = 33.16^\circ \\ \theta_{13} = 16.92^\circ \\ \theta_{21} = -35.26^\circ \\ \theta_{22} = 11.98^\circ \\ \theta_{23} = 6.93^\circ \\ \theta_{13} = -56.95^\circ \\ \theta_{23} = 74.4^\circ \\ \theta_{33} = -33.16^\circ \\ l_1 = 10.5 \text{ cm} \\ l_2 = 10.96 \text{ cm} \\ l_3 = 7.24 \text{ cm} \end{cases} \quad \text{case I,}$$

$$\begin{cases} x = 0 \\ y = 5 \text{ cm} \\ z = 5 \text{ cm} \\ \alpha = 20^\circ \\ \beta = 20^\circ \\ \gamma = 20^\circ \end{cases} \Rightarrow \begin{cases} \theta_{11} = 4.69^\circ \\ \theta_{12} = 36.13^\circ \\ \theta_{13} = 35.36^\circ \\ \theta_{21} = -36.79^\circ \\ \theta_{22} = -1.25^\circ \\ \theta_{23} = 19.02^\circ \\ \theta_{13} = -55.74^\circ \\ \theta_{23} = 71.26^\circ \\ \theta_{33} = -39.45^\circ \\ l_1 = 11.13 \text{ cm} \\ l_2 = 12.56 \text{ cm} \\ l_3 = 9.19 \text{ cm} \end{cases} \quad \text{case II,}$$

where x, y and z indicate the location of the origin of the moving coordinate frame, with respect to the base platform coordinate frame. Moreover, α, β and γ are the Euler angles of the moving coordinate frame, which specify its orientation. The lengths, as well as the spin, of each leg are also provided.

Forward Pose Solution

In the forward pose procedure, the location and orientation of the moving platform coordinate frame, with respect to the base coordinate frame, namely ${}^B_P T$, must be obtained, having active joint variables. A traditional method to solve the forward pose of the introduced mechanism, as adopted in [7], is to derive ${}^B_P T$ through each leg and equate them. That is:

$$({}^B_P T)_1 = ({}^B_P T)_2 = ({}^B_P T)_3, \tag{14}$$

where $({}^B_P T)_i$ is obtained through the ith leg. (See Figure 3 for the leg's numbering.) Each ${}^B_P T$ has six Denavit-Hartenberg parameters, θ_1, θ_2, θ_3, ϕ_1, ϕ_2 and l. Since θ_1 and θ_2 are known in the forward pose procedure, for each leg, θ_3, ϕ_1, ϕ_2 and l are unknowns. Therefore, there are twelve unknowns. Also by equating two transformation matrices, six independent equations will be available. Thus, since Equation 14 leads to the following two equations, there exist twelve equations.

$$\begin{cases} ({}^B_P T)_1 = ({}^B_P T)_2, \\ ({}^B_P T)_2 = ({}^B_P T)_3. \end{cases} \tag{15}$$

Therefore, twelve nonlinear equations obtained from Equation 15 must be solved for the twelve unknowns, employing numerical methods like Newton-Raphson. However, in this article, to solve the forward pose problem, a new method, differing from the traditional approach, is introduced and used. In this method, instead of solving twelve nonlinear equations, only three nonlinear equations with less nonlinearity have to be solved. Therefore, the proposed method is computationally more efficient. The introduced method is explained in the following. In Figure 8, the locations of the leg-platform connection points, LEP, are shown schematically.

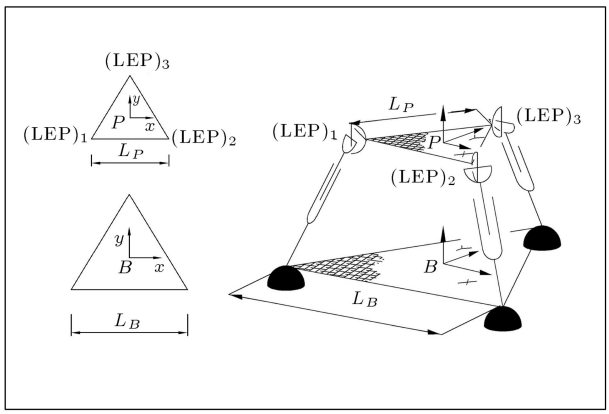

Figure 8. Schematic of LEP points used in the forward pose solution procedure.

The coordinate for $(\mathrm{LEP})_i i = 1 \cdots 3$ are as follows: The $(\mathrm{LEP})_i i = 1 \cdots 3$ are as follows:

$$(\mathrm{LEP})_1 =$$

$$\begin{bmatrix} 0.866 l_1 \cos(\theta_{11}) \cos(\theta_{21}) - 0.5 l_1 \sin(\theta_{11}) \cos(\theta_{21}) \\ \quad - 0.5001 L_B \\ 0.5 l_1 \cos(\theta_{11}) \cos(\theta_{21}) + 0.866 l_1 \sin(\theta_{11}) \cos(\theta_{21}) \\ \quad - 0.2887 L_B \\ l_1 \sin(\theta_{21}), \end{bmatrix},$$

$$(\mathrm{LEP})_2 =$$

$$\begin{bmatrix} -0.866 l_2 \cos(\theta_{12}) \cos(\theta_{22}) - 0.5 l_2 \sin(\theta_{12}) \cos(\theta_{22}) \\ \quad - 0.5001 L_B \\ 0.5 l_2 \cos(\theta_{12}) \cos(\theta_{22}) - 0.866 l_2 \sin(\theta_{12}) \cos(\theta_{22}) \\ \quad - 0.2887 L_B \\ l_2 \cos(\theta_{22}), \end{bmatrix},$$

$$(\mathrm{LEP})_3 = \begin{bmatrix} l_3 \sin(\theta_{13}) \cos(\theta_{23}) \\ -l_3 \cos(\theta_{13}) \cos(\theta_{23}) + 0.5774 L_B \\ l_3 \sin(\theta_{23}) \end{bmatrix}. \quad (16)$$

Having θ_2 and θ_1 for each leg, to find $(\mathrm{LEP})_i i = 1 \cdots 3$, the length of each leg should be evaluated. Since the platform is rigid, the distance between the pair, $((\mathrm{LEP})_i, (\mathrm{LEP})_j)$, for $i, j = 1 \cdots 3$ and $i \neq j$ has to always be constant and equal to l_p. These restrictions constraints result in:

$$\begin{cases} \|(\mathrm{LEP})_1 (\mathrm{LEP})_2\| = L_P \Rightarrow l_1^2 + l_2^2 + 2 c_{11} l_1 l_2 \\ \qquad\qquad + c_{21} l_1 + c_{31} l_2 = c_{41} \\ \|(\mathrm{LEP})_1 (\mathrm{LEP})_3\| = L_P \Rightarrow l_1^2 + l_3^2 + 2 c_{21} l_1 l_3 \\ \qquad\qquad + c_{22} l_1 + c_{32} l_3 = c_{42} \\ \|(\mathrm{LEP})_2 (\mathrm{LEP})_3\| = L_P \Rightarrow l_2^2 + l_3^2 + 2 c_{31} l_2 l_3 \\ \qquad\qquad + c_{23} l_2 + c_{33} l_3 = c_{43} \end{cases} \quad (17)$$

where c_{ij} for $i = 1 \cdots 3, j = 1 \cdots 3$ are constant. Therefore, for the forward pose problem, one can obtain l_1, l_2 and l_3 by employing a numerical method like Newton-Raphson to solve Equation 17. Solving the nonlinear equations presented in Equation 17, in comparison to solving the twelve nonlinear equations derived by the traditional method, is easier and more computationally efficient. Equation 17 is solved numerically in the following for a case study. In Figures 9a, 9b and 9c, the variation of θ_{11}, θ_{21} and θ_{12}, θ_{22} and θ_{13}, θ_{23}, with respect to time, are shown, respectively. In Figure 10, the variations of l_1, l_2 and l_3, with respect to time, obtained according to the above procedure, are shown.

It is to be noted that, in order to complete the forward pose problem, ${}^B_P T$ has to be specified, as done in the following. Having the length and orientation of each leg, the unit vector in the direction of $(X_6)_1$, shown in Figure 11, in the base coordinate frame, which

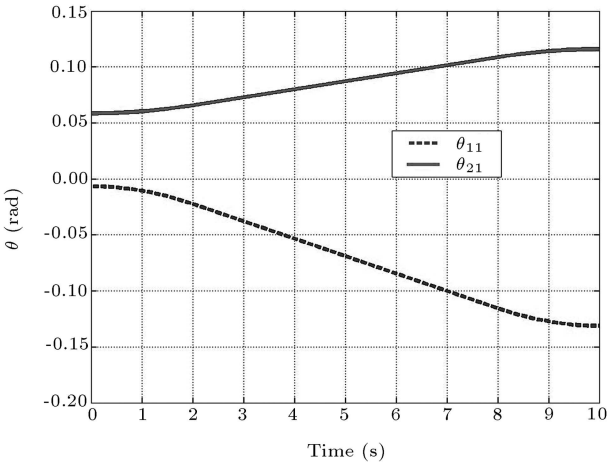

Figure 9a. The variations of the first leg's active variables with respect to time in the forward pose procedure.

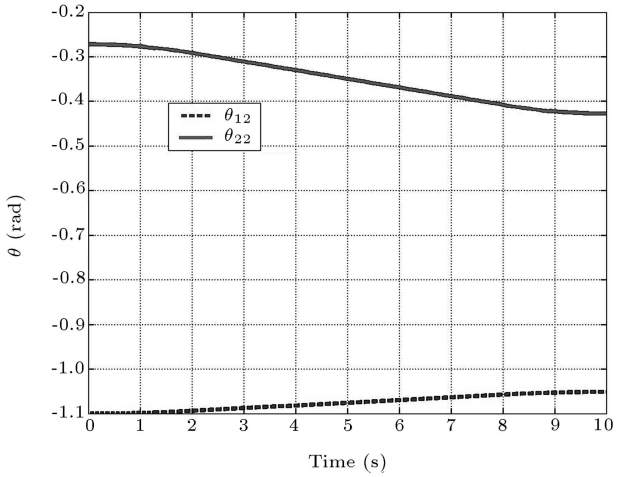

Figure 9b. The variations of the second leg's active variables with respect to time in the forward pose procedure.

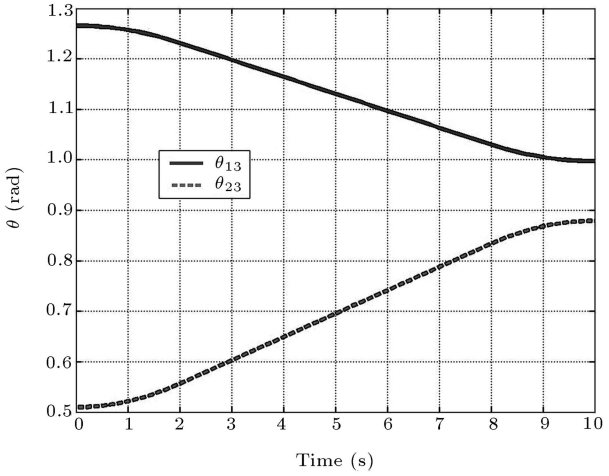

Figure 9c. The variations of the third leg's active variables with respect to time in the forward pose procedure.

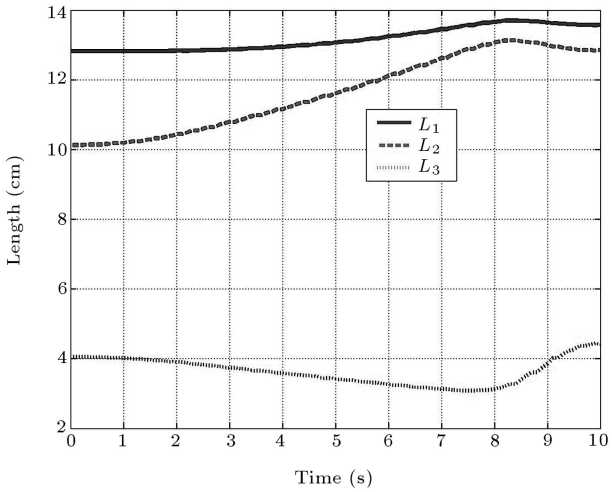

Figure 10. The variations of the lengths of the legs in the forward pose procedure.

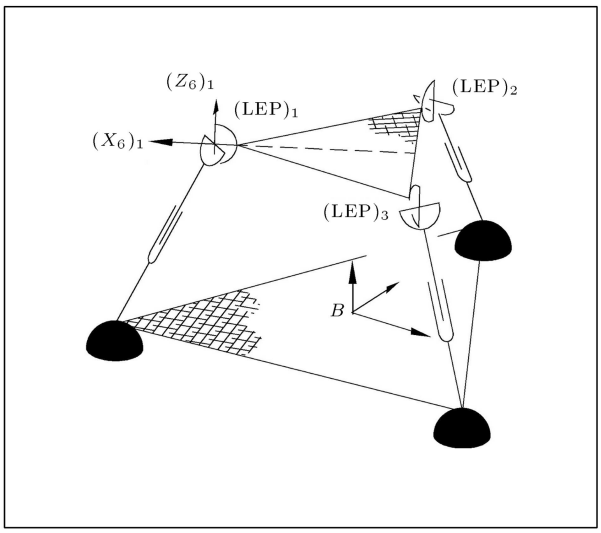

Figure 11. Schematic of the $(X_6)_1$ used in forward pose procedure.

is called ${}^{B}(X_6)_1$, is:

$$
{}^{B}(X_6)_1 = \frac{\begin{bmatrix} \frac{x_{(\mathrm{LEP})_2}+x_{(\mathrm{LEP})_3}}{2} \\ \frac{y_{(\mathrm{LEP})_2}+y_{(\mathrm{LEP})_3}}{2} \\ \frac{z_{(\mathrm{LEP})_2}+z_{(\mathrm{LEP})_3}}{2} \end{bmatrix} + \begin{bmatrix} x_{(LEP)_1} \\ y_{(LEP)_1} \\ z_{(LEP)_1} \end{bmatrix}}{l_p \frac{\sqrt{3}}{2}}
$$

$$
= \begin{bmatrix} m_1 \\ m_2 \\ m_3 \end{bmatrix}, \tag{18}
$$

where $x_{(\mathrm{LEP})_i}$, $y_{(\mathrm{LEP})_i}$ and $z_{(\mathrm{LEP})_i}$ for $i = 1 \cdots 3$ are the x, y and z components of the position of $(\mathrm{LEP})_i$, respectively. The ${}^{B}(X_6)_1$, given in Equation 18, can be expressed in the coordinate frame by multiplying it with ${}^{3}_{B}R = ({}^{B}_{3}R)^{-1}$ as:

$$
{}^{3}(X_6)_1 = {}^{3}_{B}R\,{}^{B}(X_6)_1. \tag{19}
$$

Also, ${}^{3}(X_6)_1$ is equal to the first column of $({}^{3}_{6}R)_1 = ({}^{3}_{4}R)_1({}^{4}_{5}R)_1({}^{5}_{6}R)_1$, which is:

$$
{}^{3}_{6}R_1 = ({}^{3}_{4}R^{4}_{5}R^{5}_{6}R)_1 =
$$

$$
\begin{bmatrix} \sin(\phi_{11})\cos(\phi_{21}) & -\sin(\phi_{11})\sin(\phi_{21}) & \cos(\phi_{11}) \\ \sin(\phi_{21}) & \cos(\phi_{21}) & 0 \\ -\cos(\phi_{11})\cos(\phi_{21}) & \cos(\phi_{11})\sin(\phi_{21}) & \sin(\phi_{11}) \end{bmatrix}. \tag{20}
$$

Equating the first columns of Equation 20 and 18, one has:

$$
m = \begin{bmatrix} m_1 \\ m_2 \\ m_3 \end{bmatrix} = \underbrace{{}^{3}(X_6)_1 = {}^{B}(X_6)_1\,{}^{3}_{B}R}_{\text{Completely known}}
$$

$$
= \begin{bmatrix} \sin(\phi_{11})\cos(\phi_{21}) \\ \sin(\phi_{21}) \\ -\cos(\phi_{11})\cos(\phi_{21}) \end{bmatrix}.
$$

So, ϕ_{11} is:

$$
\phi_{11} = \mathrm{atan2}(m_1, -m_3), \tag{21}
$$

and ϕ_{21} is:

$$
\begin{aligned}
&\phi_{21} = \mathrm{atan2}(m_2, -m_3/\cos(\phi_{11})) \qquad \text{If } \phi_{11} = 0 \text{ or } \pi, \\
&\phi_{21} = \mathrm{atan2}(m_2, m_1/\sin(\phi_{11})) \qquad \text{If } \phi_{11} \neq 0 \text{ or } \pi.
\end{aligned} \tag{22}
$$

After having ϕ_{11} and ϕ_{21}, θ_{31} must also be available to calculate ${}^{B}_{P}T$. To determine θ_{31}, the procedure employed in previous section to calculate θ_{3i} has to be used (see Equations 7 to 13). Finally, ${}^{B}_{P}T$ is:

$$
{}^{B}_{P}T = ({}^{B}_{0}T)_1({}^{0}_{3}T)_1({}^{3}_{4}T)_1({}^{4}_{5}T)^{5}_{6}T\,{}^{6}_{P}T, \tag{23}
$$

$({}^{B}_{0}T)_1$:	Known (because the location of coordinate 0 is known);
$({}^{0}_{3}T)_1$:	Known (because θ_{11} and θ_{21} are inputs and θ_{31} is specified);
$({}^{3}_{4}T)_1$:	Known (because ℓ_1 is calcualted);
$({}^{4}_{5}T, {}^{5}_{6}T)_1$:	Known (bacause ϕ_{11} and ϕ_{21} are calcualeted);
$({}^{6}_{P}T)_1$:	Known (because the location of coordinate 6 is known).

Rate Kinematics

In the inverse rate kinematics, the actuators' velocities should be calculated, having the linear velocity of the origin of the moving platform coordinate frame and the angular velocity of the moving platform. While in the forward rate kinematics, the linear velocity of the origin of the moving platform coordinate frame and the angular velocity of the moving platform should be obtained, giving the actuators' velocities.

Inverse Rate Kinematics

Before continuing, the following rule below, which will be used in this section, is introduced.

Rule I

$$s \times z = \tilde{s}.z,$$

where:

$$\tilde{s} = \begin{bmatrix} 0 & -s_z & s_y \\ s_z & 0 & -s_x \\ -s_y & s_x & 0 \end{bmatrix}.$$

That is, the cross product of vector z from the left side with vector s is equivalent to per-multiplication of the skew-symmetric matrix, $\tilde{s}$, given above, with z.

For ease of notation and referencing, unit vectors $\hat{n}$, $\hat{x}$, $\hat{h}$ and $\hat{x}$, as shown in Figure 12, are used instead of z_6, z_3, x_5 and $-z_5$, respectively. It is to be noted that prior to the inverse rate kinematics analysis, inverse pose kinematics are solved. Thus, all the above vectors are available.

The velocity of point LEP in Figure 12 is:

$$V_{\text{LEP}} = \dot{t} + \omega_P \times q, \tag{24}$$

where $\dot{t}$ is the velocity of the origin of the moving platform coordinate frame, ω_p is the angular velocity of the moving platform and q is shown in Figure 12. V_{LEP} can also be found from:

$$V_{\text{LEP}} = \dot{l}\hat{z} + \overbrace{(\omega + \omega_z)}^{\omega_l} \times l\hat{z}, \tag{25}$$

where l is the length of the leg, $\dot{l}$ is the rate of change of the leg length, with respect to time, ω_l is the leg's angular velocity, ω is the component of the leg's angular velocity along the leg's direction and ω_z is the component of the leg's angular velocity, perpendicular to the leg's direction.

Equating Equations 24 and 25 and taking the dot and cross products with $\hat{z}$, one obtains, respectively:

$$\dot{l} = \hat{z}.V_{\text{LEP}}, \tag{26}$$

$$\omega = \frac{\hat{z} \times V_{\text{LEP}}}{l}. \tag{27}$$

The angular velocity of the leg given in Equation 27 is perpendicular to the leg's direction. To completely define the leg's angular velocity, its components along the leg should also be specified, as has been done below. The cross symbol of the universal joint is shown in Figure 13.

The angular velocity of the cross symbol, ω_{CS}, is:

$$\omega_{CS} = \omega_p + \omega_n, \tag{28}$$

where ω_n is the relative angular velocity of the cross symbol, with respect to the platform, which is in the $\hat{n}$ direction, and ω_p is the angular velocity of the platform. Moreover, ω_{CS} is:

$$\omega_{CS} = \overbrace{\omega + \omega_z}^{\omega_l} + \omega_x, \tag{29}$$

where ω_x is the relative angular velocity of the universal joint symbol, with respect to the leg, which is in the $\hat{x}$ direction. Now, define k as:

$$k = \hat{n} \times \hat{h}. \tag{30}$$

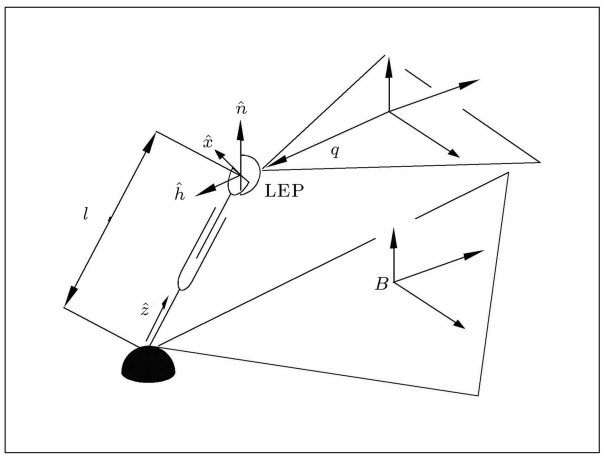

Figure 12. Definition of unit vectors $\hat{n}, \hat{z}, \hat{h}$ used in the rate kinematic analysis.

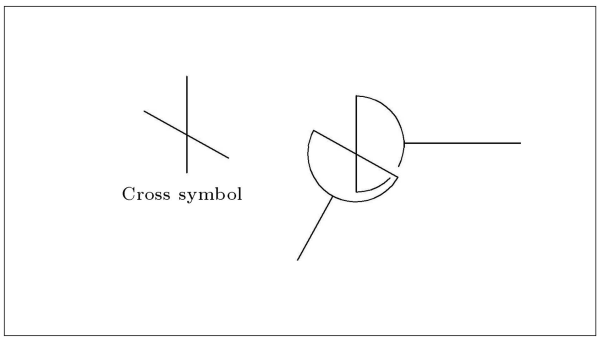

Figure 13. Schematic of the cross symbol of the universal joint.

Equating Equations 28 and 29 and taking the dot product of the result with k, defined in Equation 30, leads to:

$$k.\omega_p = k.\omega + k.\omega_z. \tag{31}$$

Therefore, from Equation 31, ω_z is:

$$\omega_z = \frac{k.(\omega_p - \omega)}{k.\hat{z}}\hat{z}. \tag{32}$$

Thus, combining Equations 27 and 32, the angular velocity of the leg is:

$$\omega_l = \frac{\hat{z} \times V_{\text{LEP}}}{l} + \left[\frac{k.\omega_p}{k.\hat{z}} + \left(k.\left(\frac{\hat{z} \times V_{\text{LEP}}}{l}\right)\frac{1}{k.\hat{z}}\right)\right]\hat{z}. \tag{33}$$

Equation 33 can be expressed in the matrix form as:

$$[\omega_l] = \begin{bmatrix} Fpv & Spv \end{bmatrix}\begin{bmatrix} \dot{t} \\ \omega_p \end{bmatrix},$$

$$Fpv = \frac{\tilde{\hat{z}}}{l} - \frac{z\hat{h}^T}{(\hat{h}.\hat{z})l}\tilde{\hat{z}},$$

$$Fsv = \left(\frac{z\hat{h}^T}{\hat{h}.\hat{z}}\right) - \frac{\tilde{\hat{z}}\tilde{q}}{l} + \frac{z\hat{h}^T}{(\hat{h}.\hat{z})l}(\tilde{\hat{z}}\tilde{q}), \tag{34}$$

where the rule introduced at the beginning of this section is adopted to derived Equation 34. After having ω_l, then, $\dot{\theta}$, $\dot{\theta}_2$ and $\dot{\theta}_3$ are:

$$(RV)^{-1}({}^0_BR)\omega_l = \dot{\theta}, \tag{35}$$

where:

$$(RV)_i = \begin{bmatrix} 0 & \sin(\theta_1) & \cos(\theta_1)\cos(\theta_2) \\ 0 & -\cos(\theta_1) & \sin(\theta_1)\cos(\theta_2) \\ 1 & 0 & \sin(\theta_2) \end{bmatrix},$$

$$\dot{\theta} = \begin{bmatrix} \dot{\theta}_1 \\ \dot{\theta}_2 \\ \dot{\theta}_3 \end{bmatrix}, \tag{36}$$

and $({}^0_BR)$ is the rotation matrix between the leg and the base coordinate frames. Equations 34 and 36 can be used for each leg and, thus, the rate of change of the active variables, $\dot{\theta}_1$ and $\dot{\theta}_2$, will be obtained. Due to space limitation, the result of the inverse rate kinematics is not provided here. However, the interested reader can find the results of several inverse rate kinematic simulations in [17].

Forward Rate Kinematics

In the forward rate kinematics, $\dot{\theta}_1$ and $\dot{\theta}_2$ of each leg are known and the platform's angular velocity and the velocity of the origin of the moving platform coordinate frame have to be obtained. Combining Equations 34 and 35, we have:

$$\dot{\theta} = \overbrace{(RV)^{-1}({}^0_BR)\omega_l \begin{bmatrix} Fpv & Spv \end{bmatrix}_i}^{A}\begin{bmatrix} \dot{t} \\ \omega_p \end{bmatrix}. \tag{37}$$

By considering the first two rows of Equation 37, one obtains:

$$\begin{bmatrix} \dot{\theta}_1 \\ \dot{\theta}_2 \end{bmatrix} = A(1:2,\ 1:6)\begin{bmatrix} \dot{t} \\ \omega_p \end{bmatrix}, \tag{38}$$

where $A(i:j,\ m:n)$ is composed of all the components of A, which are located on the ith to jth rows and the mth to nth columns. Therefore, $A(1:2,\ 1:6)$ is composed of all the components of A, which are located on the first two rows of A (note: A has 6 columns). Equation 38 can be written for each leg and combining the equations written for the three legs leads to:

$$\overbrace{\begin{bmatrix} \dot{\theta}_{11} \\ \dot{\theta}_{21} \\ \dot{\theta}_{12} \\ \dot{\theta}_{22} \\ \dot{\theta}_{13} \\ \dot{\theta}_{23} \end{bmatrix}}^{\dot{\Theta}} = \overbrace{\begin{bmatrix} A_1(1:2,\ 1:6) \\ A_2(1:2,\ 1:6) \\ A_3(1:2,\ 1:6) \end{bmatrix}}^{B}\begin{bmatrix} \dot{t} \\ \omega_p \end{bmatrix} \Rightarrow \dot{\Theta} = B\begin{bmatrix} \dot{t} \\ \omega_p \end{bmatrix}, \tag{39}$$

where A_i is the A which corresponds to the ith leg. From Equation 39, the platform's angular velocity and the velocity of the origin of the moving platform coordinate frame are:

$$\begin{bmatrix} \dot{t} \\ \omega_p \end{bmatrix} = B^{-1}\dot{\Theta}. \tag{40}$$

SINGULARITY ANALYSIS

Singular configurations for the parallel manipulators fall into two different major categories with different natures [11]. In the first category of the singular configurations, the determinant of matrix B in Equation 40 is zero, while, in other categories, the determinant of matrix B approaches to infinity. Conceptually, in the first category of the singular configurations, the parallel mechanism loses one or more DOF, while, in the second category of singular configurations, it gains one or more DOF [11]. The traditional method to obtain these configurations is to derive the determinant of matrix B, and then to find the situations in which the determinant of matrix B in Equation 39 is equal to zero or infinity. However, symbolic calculation of

the determinant of matrix B results in a complicated expression. Moreover, imposing the conditions that make this determinant equal to zero or infinity is not straightforward. To alleviate these drawbacks of the traditional method, in this section, the singular configurations of the introduced mechanism are obtained through new techniques. Also, numerical simulations available in [17] showed that, in the first category of the singular configuration, the determinant of matrix B in Equation 40 is zero, while, in the second category of the singular configuration, this determinant approaches to infinity.

First Category of the Singular Configurations

This category of singular configurations represents the situations where different solutions can exist for the inverse kinematic. Conceptually, in this category of singular configurations, the manipulator loses one or more DOF. In another words, in this category, the mechanism reached its workspace boundary or internal boundary, limiting different sub regions of the workspace.

To obtain this kind of singular configuration for our introduced mechanism, first, the Jacobian matrix of each leg should be evaluated. Having the Denavit-Hartenberg parameters for each leg from previous sections, the Jacobian Matrix and, consequently, its determinant, are calculated easily. Then, the determinant of the Jacobian Matrix is set to zero. The configurations that satisfy this condition will lead to the first category of the singular configurations and the conditions to fall into this category are as follows:

$$\det(J_i) = \ell_i^2 \sin(\theta_{2i}) \cos(\phi_{1i}),$$

$$\det(J) = 0 \Rightarrow \left\{ \begin{array}{ll} \ell_i = 0 & \text{(a)} \\ \theta_{2i} = \pm 90 & \text{(b)} \\ \phi_{1i} = \pm 90 & \text{(c)} \end{array} \right\}, \qquad (i = 1 \cdots 3). \tag{41}$$

From the above equation, it is clear that there are three different conditions for this category of singular configuration, which are discussed in detail below.

Case A $\ell_i (i = 1 \cdots 3)$: In this case, one, or more than one, leg(s) reaches its boundary. A schematic of the parallel manipulator at this singular configuration is shown in Figure 14. As can be seen from the schematic, the mechanism lost one DOF. It should be noted that, if, in Case A of the singular configuration, more than one leg has zero length, then, the condition $l_P = l_B$ exists.

Case B $\theta_{2i} = \pm 90$ $(i = 1 \cdots 3)$: In this case, Z_{1i} and Z_{3i} become colinear. Since the rotation axes for θ_1 and θ_3 are parallel, variables θ_1 and θ_3 act like each other. Thus, again, the mechanism loses one DOF. Geometrically, in this case, the leg, for which the rotation axes of θ_1 and θ_3 are parallel, will be perpendicular to the ground. A schematic of the mechanism, in this case, is shown in Figure 15. It is worth mentioning that if more than one leg wants to be perpendicular to the ground, then, the condition $l_P = l_B$ exists.

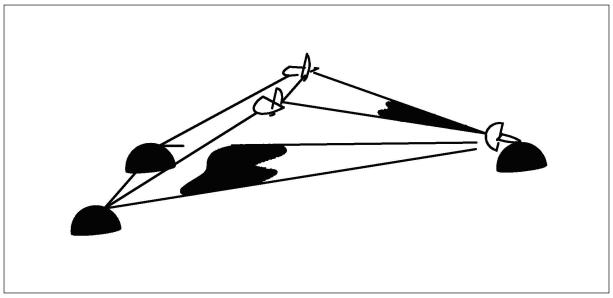

Figure 14. Schematic of the mechanism in Case A of the first category of the singular configuration.

Case C $\phi_{1i} = \pm 90$ $(i = 1 \cdots 3)$: In this case, Z_{6i} and Z_{3i} become colinear and because of the similar reason explained in Case B, again, the manipulator loses one DOF. Geometrically, in this case, the leg will be perpendicular to the moving platform. The schematic of the manipulator in this case, is shown in Figure 16. It is worth mentioning that if more than one leg wants to be perpendicular to the moving platform, then, condition $l_P = l_B$ exists.

Second Category of Singular Configurations

The second category of singular configurations occurs when the platform is movable, even when the active joints are locked. Therefore, it could be easily concluded that, in this category, the parallel manipulator gains one or more degree of freedom. From a different viewpoint, this category includes the configurations of

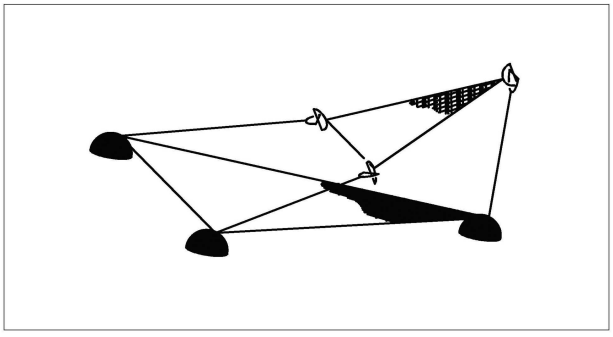

Figure 15. Schematic of the mechanism in Case B of the first category of the singular configuration.

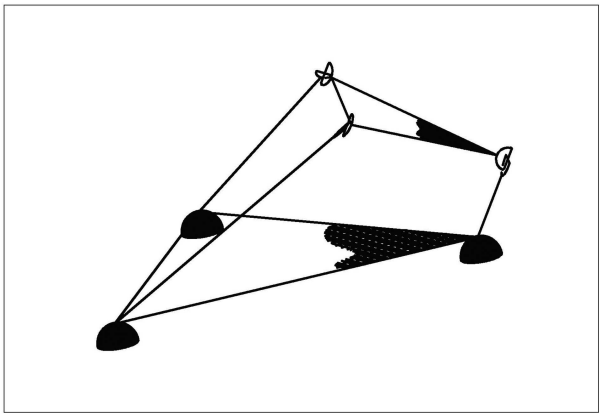

Figure 16. Schematic of the mechanism in Case C of the first category of the singular configuration.

the parallel manipulator, in which different solutions can exist for the forward kinematic problem. Based on the definition, as already stated, in this category, the parallel manipulator is movable, even if the actuators are locked. Therefore, to obtain the condition that leads to these singular configurations, first, it is assumed that the actuators are locked and, then, the requirement that makes the manipulator movable is explored.

In Figure 17, the schematic of the parallel manipulator and the angles that each leg have with the moving platform, are shown. Since the actuators are locked, points $(\text{LEP})_1$, $(\text{LEP})_2$ and $(\text{LEP})_3$ can only have velocity along their corresponding leg's direction or:

$$V_{(\text{LEP})_i} = \dot{l}_i \hat{z}_i, \tag{42}$$

where $V_{(\text{LEP})_i}$ and $\dot{l}_i$ are the velocity of $(\text{LEP})_i$ and the derivate of l_i, with respect to time, respectively. Since it is assumed that the moving platform is rigid, the velocity given in Equation 42 is feasible, provided that the projections of $V_{(\text{LEP})_i}$ and $V_{(\text{LEP})_j}$ for $i, j = 1 \cdots 3$, $i \neq 3$ along the sides of the moving triangle that is constructed by $(\text{LEP})_i$ and $(\text{LEP})_j$, be the same. These conditions result in:

$$\begin{cases} \dot{l}_1 \cos(\lambda_2) - \dot{l}_2 \cos(\lambda_3) = 0 \\ \dot{l}_2 \cos(\lambda_4) - \dot{l}_3 \cos(\lambda_5) = 0 \\ \dot{l}_3 \cos(\lambda_6) - \dot{l}_1 \cos(\lambda_1) = 0 \end{cases} \tag{43}$$

or:

$$\overbrace{\begin{bmatrix} \cos(\lambda_2) & -\cos(\lambda_3) & 0 \\ 0 & \cos(\lambda_4) & -\cos(\lambda_5) \\ -\cos(\lambda_1) & 0 & \cos(\lambda_6) \end{bmatrix}}^{M} = \begin{bmatrix} \dot{l}_1 \\ \dot{l}_2 \\ \dot{l}_3 \end{bmatrix} = \begin{bmatrix} 0 \\ 0 \\ 0 \end{bmatrix}. \tag{44}$$

From the above equation, if the determinant of matrix M is not equal to zero, that is, $|M| \neq 0$, then, the only possible solution is $\dot{l}_i = 0$ for $i = 1 \cdots 3$. That is, by locking the actuators, if the configuration of the manipulator is such that $|M| \neq 0$, then, no movement is possible. However, if the determinate of matrix M in Equation 44 is equal to zero, that is, $|M| = 0$, then, there can be non-zero values for $\dot{l}_i$ for $i = 1 \cdots 3$. That is, although the actuators are locked, the platform can still move. Therefore, the manipulator will be in the second category of singular configurations if:

$$|M| = 0. \tag{45}$$

Considering the definition of matrix M given in Equation 44, the condition $|M| = 0$ is:

$$\begin{aligned} |M| = 0 \Rightarrow & \cos(\lambda_1)\cos(\lambda_3)\cos(\lambda_5) \\ & = \cos(\lambda_2)\cos(\lambda_4)\cos(\lambda_6). \end{aligned} \tag{46}$$

From Figure 18, the following relation between $\cos(\lambda_1)$, $\cos(\alpha_1)$ and $\cos(\beta_1)$ exists:

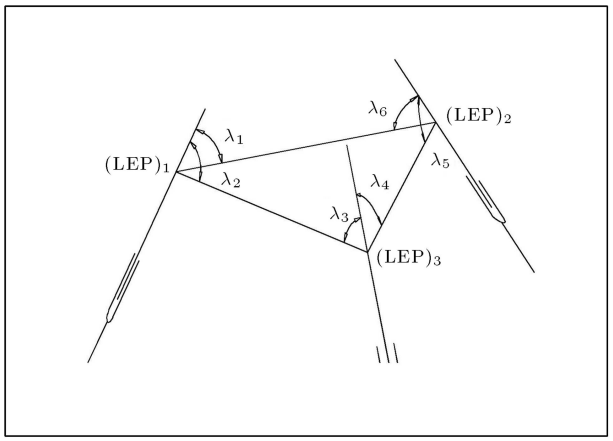

Figure 17. The schematic of the angle of the sides of the moving platform with the legs used in finding the second category of the singular configuration.

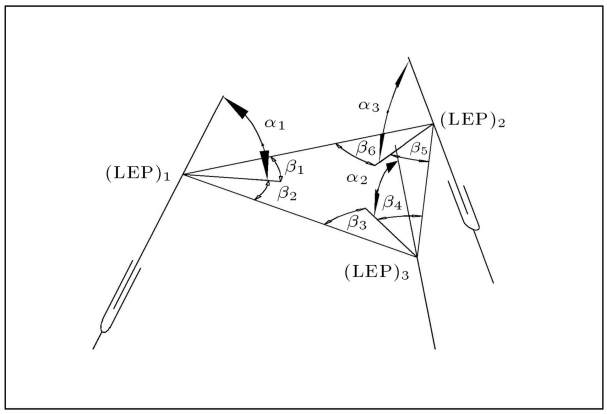

Figure 18. The schematic of the angles of the projection of each leg's extension on the moving platform.

$$\cos(\lambda_1) = \cos(\alpha_1)\cos(\beta_1). \quad (47)$$

Writing the same relation as the one given in Equation 47 for $\cos(\lambda_2)$, $\cos(\lambda_3)$, $\cos(\lambda_4)$, $\cos(\lambda_5)$ and $\cos(\lambda_6)$ and substituting the results in Equation 46, yields:

$$\cos(\beta_1)\cos(\beta_3)\cos(\beta_5) = \cos(\beta_2)\cos(\beta_4)\cos(\beta_6). \quad (48)$$

Therefore, the manipulator will be in the second category of the singular configuration, provided that β_i for $i = 1 \cdots 6$, as given in Figure 18, satisfies the condition given in Equation 48.

CONCLUSION

In this article, a new 6 Degree-Of-Freedom (DOF) parallel manipulator, which has three legs, with partial spherical actuators, was studied. Each leg of this mechanism was composed of spherical, prismatic and universal joints in a serial manner.

In the inverse pose kinematics, active joint variables were calculated with no need for evaluation of the passive join variables. In the forward pose kinematics, instead of solving twelve nonlinear equations, which would have to be solved if the traditional approach were adopted, only three nonlinear equations with less nonlinearity were solved. Moreover, the inverse and forward rate kinematics were analyzed and closed form relations between actuator rates and the platform's linear and angular velocities were derived. Furthermore, two different categories of singular configurations for mechanisms with different natures were introduced. In the first category, the mechanism loses one or more DOF(s), while, in the second category, it gains one or more DOF(s).

It is clear that each spherical actuator has three inputs. Since there are three spherical joints in the mechanism, there can be up to nine independent inputs for the mechanism, while, by only six independent inputs, the location and orientation of a 6 DOF manipulator is completely specified. Thus, there are several different ways to actuate the introduced mechanism [13] and, in this article, only one way was studied. Assuming fully actuated spherical joints and switching from one actuation way to another would expand the mechanism workspace and might make the workspace singularity free, which can be a subject for future research.

REFERENCES

1. Stewart, D. "A platform with six degree of freedom manipulator", *Proceeding of the Institute of Mechanical Engineering*, **180**(15), pp. 371-38 (1965).
2. Hunt, K.H. "Structural kinematics of in-parallel-actuated robot arms", *ASME Journal of Mechanism Design*, **105**, pp. 705-712 (1983).
3. Romiti, A. and Sorli, M. "A parallel 6-DOF manipulator for cooperative work between robots in debarring", *Proceeding of the 23rd International Symposium on Industrial Robots*, Barcelona, Spain, pp. 437-442 (1992).
4. Behi, F. "Kinematics analysis for a six-degree-of-freedom 3-PRPS parallel manipulator", *IEEE Transactions of Robotics and Automation*, **4**, pp. 561-565 (1988).
5. Hudgens, J. and Tear, D. "A fully-parallel six degree-of-freedom micromanipulator: Kinematics analysis and dynamic model", *Proceeding of the 20th Biennial ASME Mechanisms Conference*, **15**(3), pp. 29-38 (1988).
6. Jongwon, K., Jae, H.C., Jin, K.S. and Park, F.C. "A new parallel mechanism enabling continuous 360-degree spinning plus three-axis translational motional motions", *Proceeding of IEEE International Conference of Robotics and Automation*, Seoul, Korea, pp. 3274-3279 (2001).
7. Williams II, R.L. and Polling, D.B. "Spherically actuated platform manipulator", *Journal of Robotics Systems*, **18**(3), pp. 147-157 (2001).
8. Zhang, C.D. and Song, S.M. "Forward kinematics of a class of parallel (Stewart) platform with closed-form solution", *Journal of Robotics Systems*, **9**(1), pp. 32-44 (1992).
9. Do, W.Q.D. and Yang, D.C.H. "Inverse dynamic analysis and simulation of a platform type robot", *Journal of Robotics Systems*, **5**(3), pp. 209-227 (1989).
10. Daniali, H.R.M., Zsombor-Murray, P.J. and Angeles, J. "The kinematics of spatial double-triangle parallel manipulator", *ASME Journal of Mechanical Design*, **115**(4), pp. 658-661 (1995).
11. Gosselin, C. and Angeles, J. "Singularity analysis of closed-loop kinematic chains", *IEEE Transactions on Robotics and Automation*, **6**(3), pp. 281-290 (1990).
12. Vakil, M., Pendar, H. and Zohoor, H. "A novel six degree-of-freedom parallel manipulator with three legs", *Proceeding of the 28th ASME Biennial Mechanism and Robotics Conference*, Salt Lake City, USA, pp. 603-610 (2004).
13. Vakil, M., Pendar, H. and Zohoor, H. "On the different actuation's ways of the spherically actuated platform manipulator", *Proceeding of the 29th Biennial Mechanism and Robotics Conference*, Long Beach, USA, pp. 785-792 (2005).
14. Lee, K.M., Roth, R.B. and Zhou, Z. Dynamics and Control of a Ball-Joint-Like Variable Reluctance Spherical Motor, ASME Journal of Dynamics System, Measurement and Control, 118 (1), pp. 29-40 (1996).
15. Wang, J., Wang, W., Jewell, G.W. and Hoew, D. "Novel spherical permanent magnet actuator with three degrees-of-freedom", *IEEE Transactions on Magnetics*, **34**(4), pp. 2078-2080 (1998).

16. Pendar, H., Vakil, M., Fotouhi, R. and Zohoor, H. "Kinematic analysis of the spherically actuated platform manipulator", *IEEE International Conference on Robotics and Automation*, Roma, Italy, pp. 175-180 (2007).
17. Vakil, M. "Kinematics and dynamic analysis of the spherically actuated platform manipulator", M.S. thesis, Sharif University of Technology, Tehran, Iran (2003).

APPENDIX

$$({}^{0}_{B}T)_1 = \begin{bmatrix} \cos(-30) & -\sin(-30) & 0 & L_b tg(30) \\ \sin(-30) & \cos(-30) & 0 & 0 \\ 0 & 0 & 1 & 0 \\ 0 & 0 & 0 & 1 \end{bmatrix},$$

$$({}^{0}_{B}T)_2 = \begin{bmatrix} \cos(-150) & -\sin(-150) & 0 & L_b tg(30) \\ \sin(-150) & \cos(-150) & 0 & 0 \\ 0 & 0 & 1 & 0 \\ 0 & 0 & 0 & 1 \end{bmatrix},$$

$$({}^{0}_{B}T)_3 = \begin{bmatrix} \cos(90) & -\sin(90) & 0 & L_b tg(30) \\ \sin(90) & \cos(90) & 0 & 0 \\ 0 & 0 & 1 & 0 \\ 0 & 0 & 0 & 1 \end{bmatrix},$$

$$({}^{P}_{6}T)_1$$

$$= \begin{bmatrix} \cos(-150) & -\sin(-150) & 0 & -L_P \sin(30) \\ \sin(-150) & \cos(-150) & 0 & -L_P tg(30)/2 \\ 0 & 0 & 1 & 0 \\ 0 & 0 & 0 & 1 \end{bmatrix},$$

$$({}^{P}_{6}T)_2$$

$$= \begin{bmatrix} \cos(-30) & -\sin(-30) & 0 & L_P \sin(30) \\ \sin(-30) & \cos(-30) & 0 & -L_P tg(30)/2 \\ 0 & 0 & 1 & 0 \\ 0 & 0 & 0 & 1 \end{bmatrix},$$

$$({}^{P}_{6}T)_3 = \begin{bmatrix} \cos(90) & -\sin(90) & 0 & 0 \\ \sin(90) & \cos(90) & 0 & L_P tg(30) \\ 0 & 0 & 1 & 0 \\ 0 & 0 & 0 & 1 \end{bmatrix}.$$